

The Effect of Coupling between Translational and Torsional modes, A Case Study

L.J. Aurelius^a, A.W. Rofai^a, J.D. Holmes^b

^aWindtech Consultants Pty.Ltd., Arncliffe, New South Wales, Australia

^bJDH Consulting, Mentone, Victoria, Australia

Introduction

The use of the High Frequency Base Balance (HFBB) [Tschanz *et al* 1983, Boggs *et al* 1989] technique to determine the overall structural wind loads, and responses such as displacements, velocities and accelerations, on tall buildings at the design stage is a well established one. However, when dealing with tall buildings that have coupled modes of vibration, where there are simultaneous sway and twist motions, there are apparently still significant differences in the methods used for dealing with this structural phenomenon.

This paper will examine and compare two methods used to determine the base moment coefficients, translational accelerations and rotational accelerations for a typical building that exhibits coupled modes of vibration. These methods are applicable only to the resonant components of the base moment responses and have no effect on the mean or background components.

Methodology

For the two methods described below, component weightings and mode Shape corrections for sway and twist were made according to those recommended in Holmes (2003). These are as follows:

$$\begin{aligned}\eta_{1x}^2 &= \hat{\phi}_{1x}^2 \left(\frac{4}{1+3\beta_{1x}} \right); & \eta_{1y}^2 &= \hat{\phi}_{1y}^2 \left(\frac{4}{1+3\beta_{1y}} \right); & \eta_{1\theta}^2 &= \hat{\phi}_{1\theta}^2 \left(\frac{1}{1+2\beta_{1\theta}} \right); \\ \eta_{2x}^2 &= \hat{\phi}_{2x}^2 \left(\frac{4}{1+3\beta_{2x}} \right); & \eta_{2y}^2 &= \hat{\phi}_{2y}^2 \left(\frac{4}{1+3\beta_{2y}} \right); & \eta_{2\theta}^2 &= \hat{\phi}_{2\theta}^2 \left(\frac{1}{1+2\beta_{2\theta}} \right); \\ \eta_{3x}^2 &= \hat{\phi}_{3x}^2 \left(\frac{4}{1+3\beta_{3x}} \right); & \eta_{3y}^2 &= \hat{\phi}_{3y}^2 \left(\frac{4}{1+3\beta_{3y}} \right); & \eta_{3\theta}^2 &= \hat{\phi}_{3\theta}^2 \left(\frac{1}{1+2\beta_{3\theta}} \right);\end{aligned}$$

Method 1: Correction of Measured Spectra.

In this method, the auto spectral densities, shown below, of the three output signals proportional to M_x , M_y and M_z , are determined. Then the spectra of the generalized forces for the three lower modes are determined by linear weighting and summing of the resulting spectral densities.

$$\begin{aligned}S_{F1}(n) &= \eta_{1x}^2 (1/h^2) S_{My}(n) + \eta_{1y}^2 (1/h^2) S_{Mx}(n) + \eta_{1\theta}^2 S_{Mz}(n) \\ S_{F2}(n) &= \eta_{2x}^2 (1/h^2) S_{My}(n) + \eta_{2y}^2 (1/h^2) S_{Mx}(n) + \eta_{2\theta}^2 S_{Mz}(n) \\ S_{F3}(n) &= \eta_{3x}^2 (1/h^2) S_{My}(n) + \eta_{3y}^2 (1/h^2) S_{Mx}(n) + \eta_{3\theta}^2 S_{Mz}(n)\end{aligned}$$

Method 2: Correction of Time Histories.

Errors in neglecting any correlation between the three measured moments in Method 1, are avoided by directly forming the time histories (see below) of the generalized forces for each mode, by weighting the time histories of the measured base moments, and then calculating the spectral densities from the resultant time series.

$$F_1(t) = \eta_{1x} (1/h) M_y(t) + \eta_{1y} (1/h) M_x(t) + \eta_{1\theta} M_z(t)$$

$$F_2(t) = \eta_{2x} (1/h) M_y(t) + \eta_{2y} (1/h) M_x(t) + \eta_{2\theta} M_z(t)$$

$$F_3(t) = \eta_{3x} (1/h) M_y(t) + \eta_{3y} (1/h) M_x(t) + \eta_{3\theta} M_z(t)$$

Experimental Setup

Tests were performed on a tall building model (scale 1:250) placed in Windtech's Blockage Tolerant Boundary Layer Wind Tunnel. The tower section of the model was attached to Windtech's High Frequency Base Balance rig. The axis convention adopted for the tests is described in Figure 1. A sample rate of 512 samples per second was used, with a sample time of 64 seconds. This was more than adequate for the given full-scale frequency band, which for the first three modes ranged between 0.148Hz and 0.204Hz.

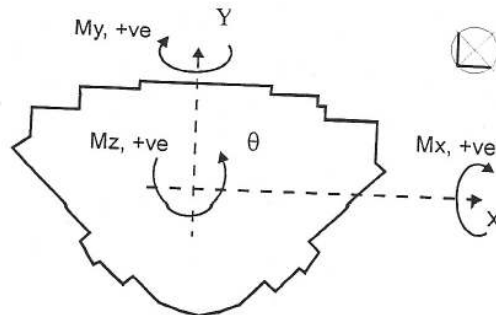


Figure 1: Axis Convention for the model

Results

The base moment coefficient data was calculated for each methodology. The base moment coefficients are defined as follows:

$$C_{Mx} = \frac{M_x}{\frac{1}{2} \rho V^2 b h^2} \quad C_{My} = \frac{M_y}{\frac{1}{2} \rho V^2 b h^2} \quad C_{Mz} = \frac{M_z}{\frac{1}{2} \rho V^2 b^2 h}$$

In addition to the base moment coefficient data for each axis, combined translational accelerations and rotational velocities at the tallest occupiable floor of the building were also calculated. Comparisons of the moment coefficients for each axis, along with a comparison of the combined translational accelerations and rotational velocities, are shown in Figures 2 to 6.

Base Bending Moment Coefficients about the X and Z axes.

The first and third modes of vibration for the tall building are highly coupled modes involving translational movement along the X-axis and rotation about the Z-axis (torsion). From Figures 2 and 4 it is apparent that the base moment coefficients obtained by Method 1 are generally larger than those obtained by Method 2 for these 2 modes. The differences in the results can be attributed to Method 1 not accounting for the effect of correlation between the 3 components of the base moments. Another reason for the differences between the two methods may be due to additional cross modal energy dissipation that is not accounted for in Method 1.

Base Bending Moment Coefficients about the Y axis.

The second mode of vibration for the building examined is a purely translational mode about the Y-axis. Results for the base moment coefficients for motion about the Y-axis is shown on Figure 3. As expected, due to the negligible amount of coupling within this mode, the results from Methods 1 and 2 are very similar.

Combined Translational Accelerations and Rotational Velocities.

Figure 5 presents the maximum combined (X, Y and Z axis) 5 year return standard deviation and 10 year return peak translational accelerations, whilst Figure 6 shows the 10 year return peak rotational velocities. These results are all based on critical damping ratios of 1%. The results obtained from Method 1 are higher than those obtained from Method 2. Again, the approximations incorporated into the methodology of Method 1, along with the energy dissipation between the coupled modes which is accounted for in Method 2, are factors that have contributed to the reductions in the accelerations from Method 2 over those derived using Method 1.

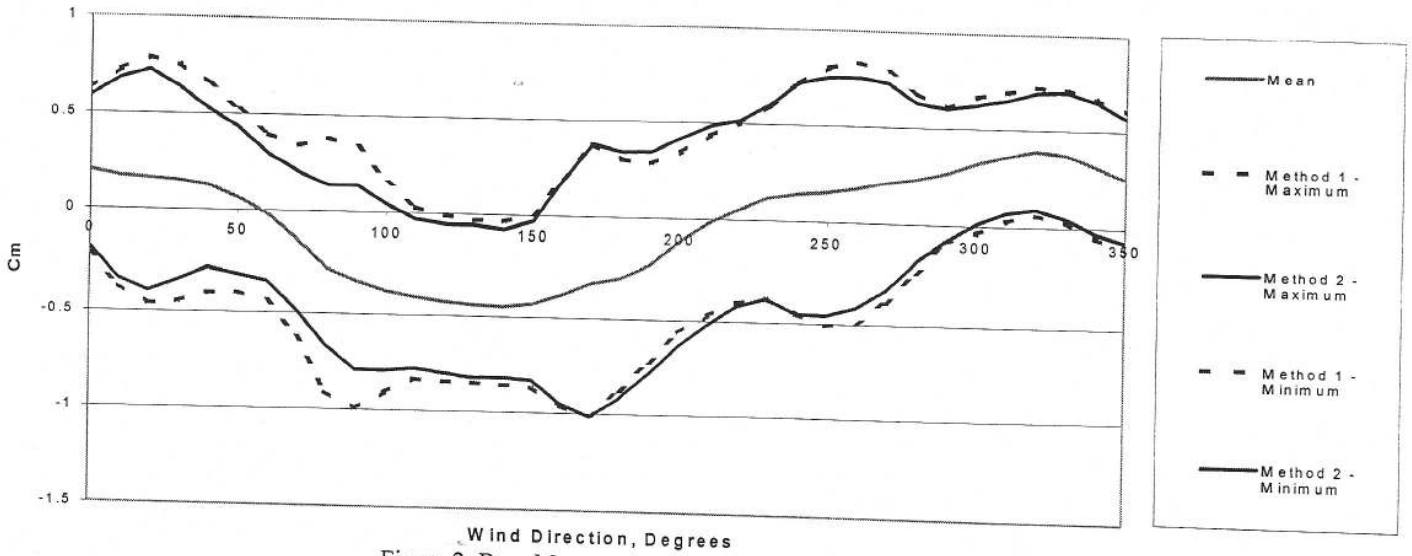
Conclusions

It is apparent that the methodology presented in Method 1 overestimates the base bending moment coefficients and accelerations for highly coupled modes. This may be due to Method 1 not accounting for the effect of correlation between the different components of the base moments. Method 2 can account for the loss of energy due to cross modal energy dissipation in highly coupled modes.

References

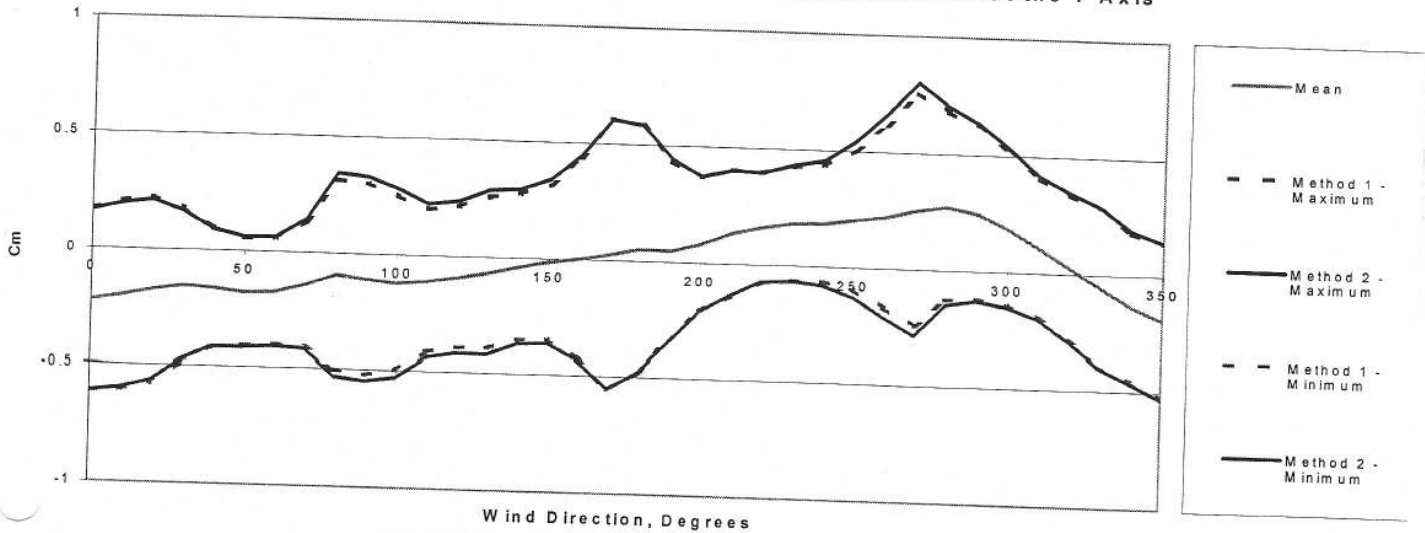
- P.A. Irwin and J.Xie. Wind loading and serviceability of tall buildings in tropical cyclone regions. 3rd Asia-Pacific Symposium on Wind Engineering, Hong Kong, 1993.
- J.D.Holmes. Mode Shape Corrections for Sway and Twist Modes, 10th Australasian Wind Engineering Society Workshop, Sydney, February 6-7, 2003
- T.Tschanz and A.G.Davenport. The Base Balance Technique for the determination of dynamic wind loading. *JWEIA* Vol. 13, 1983, pp 429-439
- D.W.Boggs and J.A.Peterka. Aerodynamic model tests of tall buildings. *Journal of Engineering Mechanics*, ASCE, Vol. 115, pp618-635, 1989

Comparison of Base Bending Moment Coefficients About the X Axis



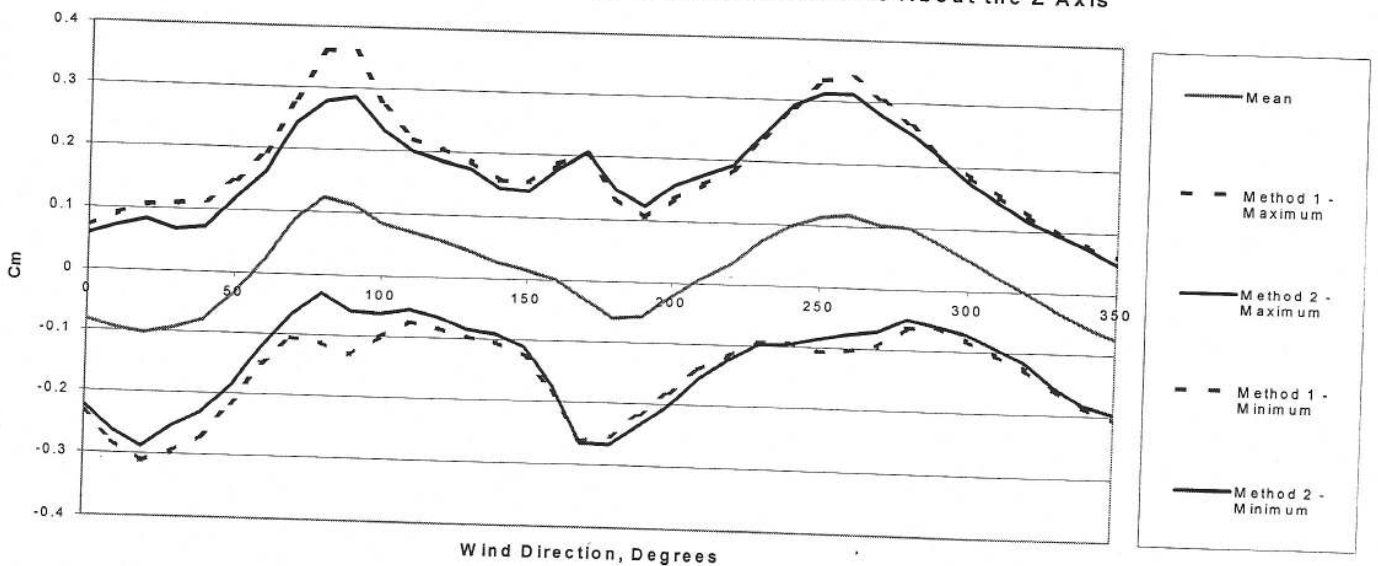
Wind Direction, Degrees
Figure 2: Base Moment Coefficients about the X axis

Comparison of Base Bending Moment Coefficients About the Y Axis



Wind Direction, Degrees
Figure 3: Base Moment Coefficients about the Y axis

Comparison of Base Bending Moment Coefficients About the Z Axis



Wind Direction, Degrees
Figure 4: Base Moment Coefficients about the Z axis

Comparison of Translational Accelerations

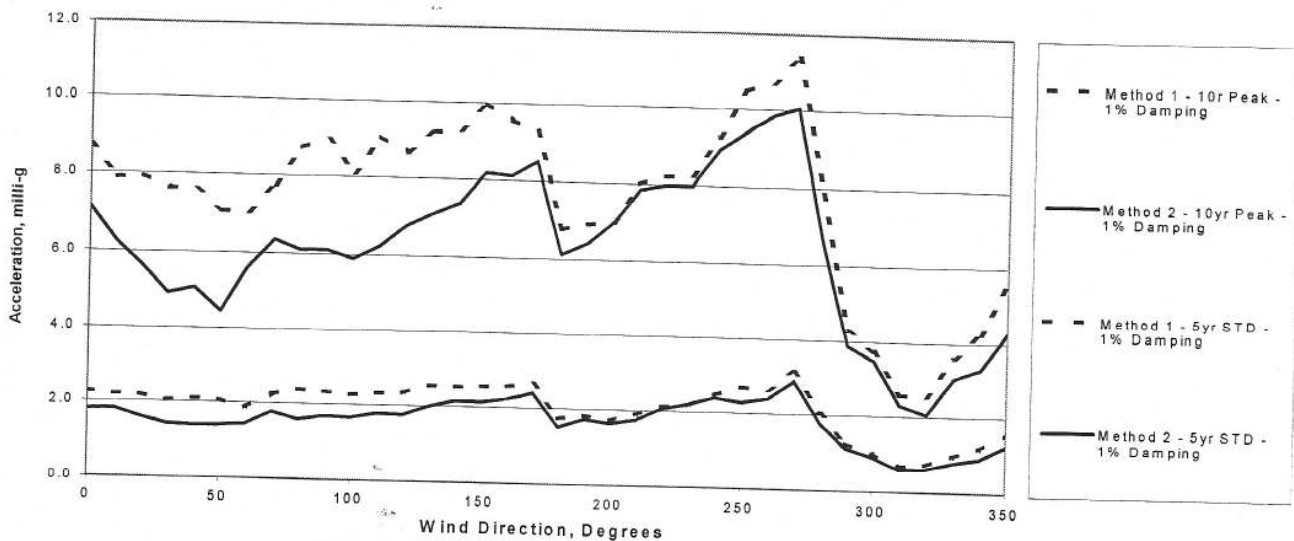


Figure 5: Combined Translational Accelerations

Comparison of Rotational Velocities



Figure 6: Rotational Velocities